Обзор ArXiv/astro-ph, 20-24 июля 2020

От Сильченко О.К.

ArXiv: 2007.12170

Exploring AGN and Star Formation Activity of Massive Galaxies at Cosmic Noon

Jonathan Florez,[1]★ Shardha Jogee,[1] Sydney Sherman,[1] Matthew L. Stevans,[1] Steven L. Finkelstein,[1] Casey Papovich,[2] Lalitwadee Kawinwanichakij,[2,3] Robin Ciardullo,[4,5] Caryl Gronwall,[4,5] C. Megan Urry,[6,7] Allison Kirkpatrick,[8] Stephanie M. LaMassa,[9] Tonima Tasnim Ananna[10] and Isak Wold[11]

[1] *Department of Astronomy, University of Texas at Austin, Austin, TX 78712, USA*
[2] *Department of Physics and Astronomy, Texas A&M University, College Station, TX 77843, USA*
[3] *Kavli Institute for the Physics and Mathematics of the Universe, The University of Tokyo, Kashiwa, Japan 277-8583 (Kavli IPMU, WPI)*
[4] *Department of Astronomy and Astrophysics, The Pennsylvania State University, University Park, PA 16802, USA*
[5] *The Institute for Gravitation and the Cosmos, The Pennsylvania State University, University Park, PA 16802, USA*
[6] *Yale Center for Astronomy & Astrophysics, New Haven, CT 06520, USA*
[7] *Department of Physics, Yale University, PO BOX 201820,New Haven, CT 06520, USA*
[8] *Department of Physics & Astronomy, University of Kansas, Lawrence, KS 66045, USA*
[9] *Space Telescope Science Institute, 3700 San Martin Dr, Baltimore, MD 21218, USA*
[10] *Department of Physics & Astronomy, Dartmouth College, 6127 Wilder Laboratory, Hanover, NH 03755, USA*
[11] *NASA Goddard Space Flight Center, Greenbelt, MD 20771*

Построение выборок AGN и БЕЗ AGN (выборки сравнения) в Stripe82

This allows us to measure and compare the star forming properties of both samples in the same self-consistent way, unlike many other studies. We select our samples from a very large 11.8 deg^2 field where the Stripe 82X X-ray survey (LaMassa et al. 2016) and the Spitzer-HETDEX Exploratory Large Area (SHELA) IRAC survey overlap Papovich et al. (2016). Our samples have extensive multi-wavelength coverage (e.g., X-ray, UV, optical, near-to-mid-IR, and some far-IR/submillimeter) over the 11.8 deg^2 field, which corresponds to a very large comoving volume of ~ 0.3 Gpc^3 at $z = 0.5-3$. Such a large comoving volume minimizes the effects of cosmic variance and captures a large sample of rare massive galaxies ($\sim 30,000$ galaxies with $M_* > 10^{11}\ M_\odot$) and X-ray luminous AGN (~ 700 objects with $L_X > 10^{44}$ erg s^{-1}), allowing us to provide some of the strongest constraints to-date on the relation between AGN and SF activity at $z \sim 1-3$.

lize the large-area, multi-wavelength data available in the SHELA/HETDEX footprint, which consists of five photometric data sets: Dark Energy Camera (DECam) u, g, r, i, z (Wold et al. 2019), NEWFIRM K_S (Stevans et al. submitted), *Spitzer*-IRAC 3.6 and 4.5 μm (Papovich et al. 2016), *Herschel*-SPIRE far-IR/submillimeter (HerS, Viero et al. 2014) and Stripe 82X X-ray (LaMassa et al. 2016). We also utilize available J and K_S-band data from the VISTA-CFHT Stripe 82 (VICS82) Near-Infrared Survey (Geach et al. 2017) and mid-IR photometry from the WISE survey (Wright et al. 2010) to supplement this work. In the near future, optical integral-field spectroscopy between 3500 and 5000 Å of this region will be available from the Hobby Eberly Telescope Dark Energy Experiment (Hill & HETDEX Consortium 2016).

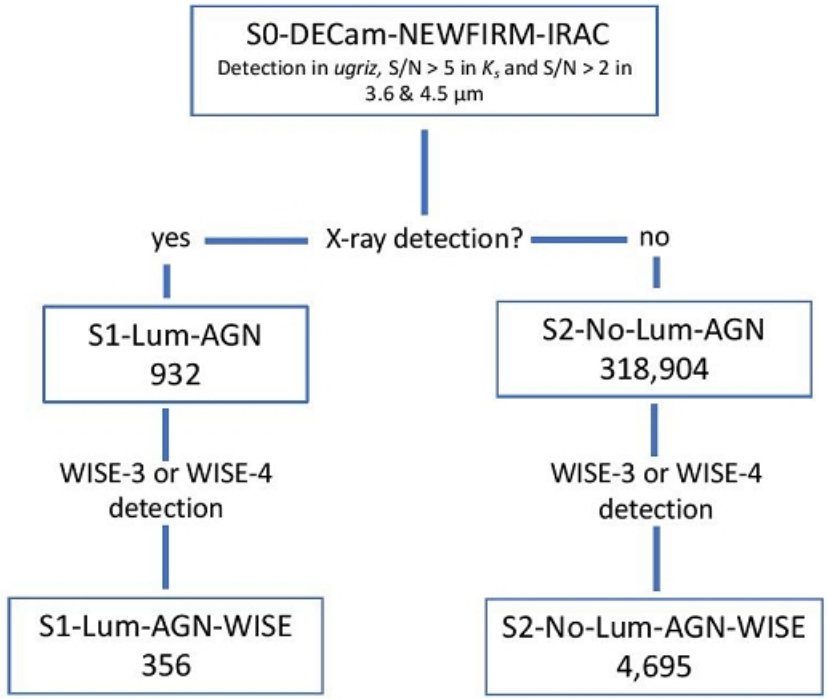

Распределение по массам

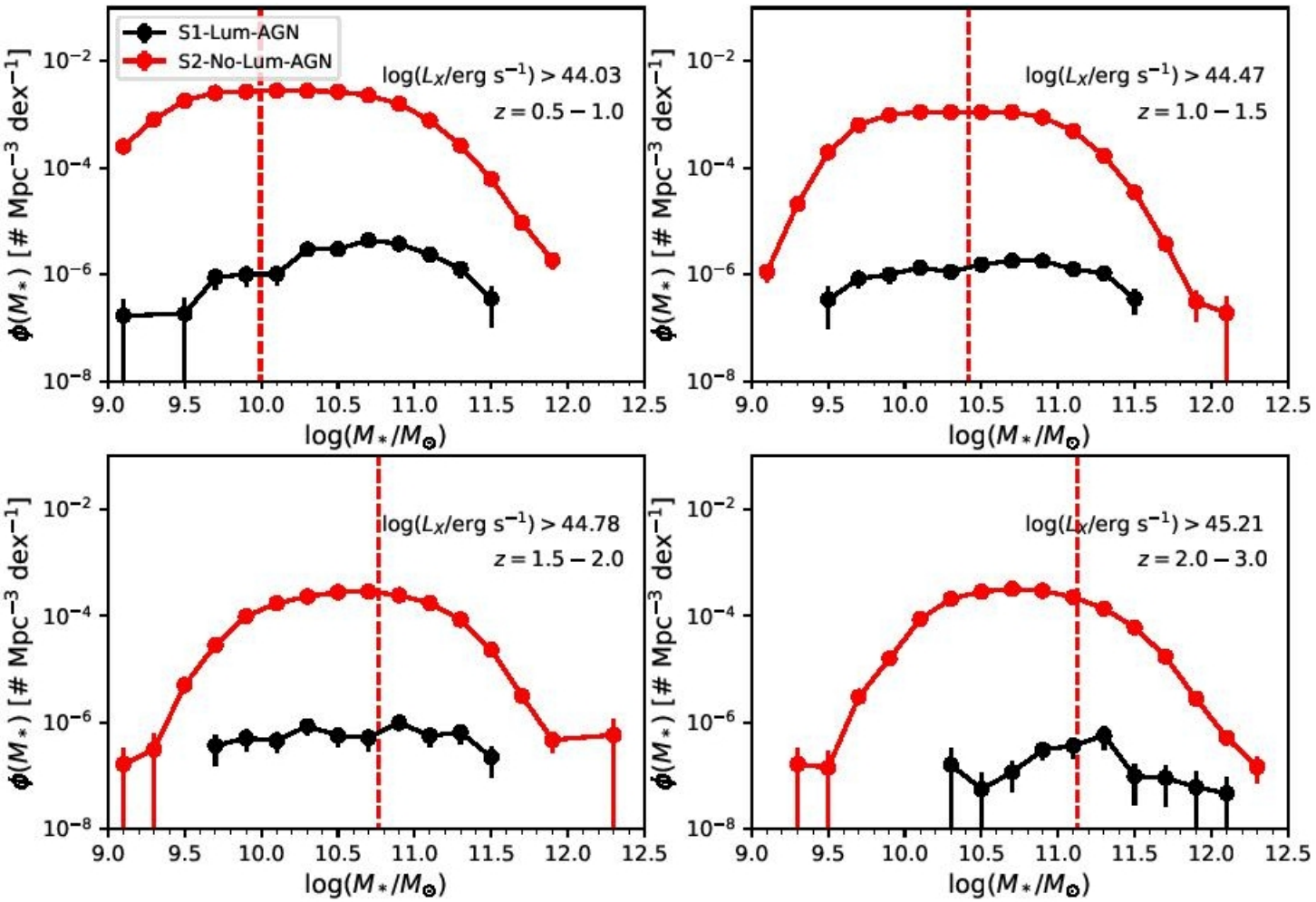

Определение SFR через SED

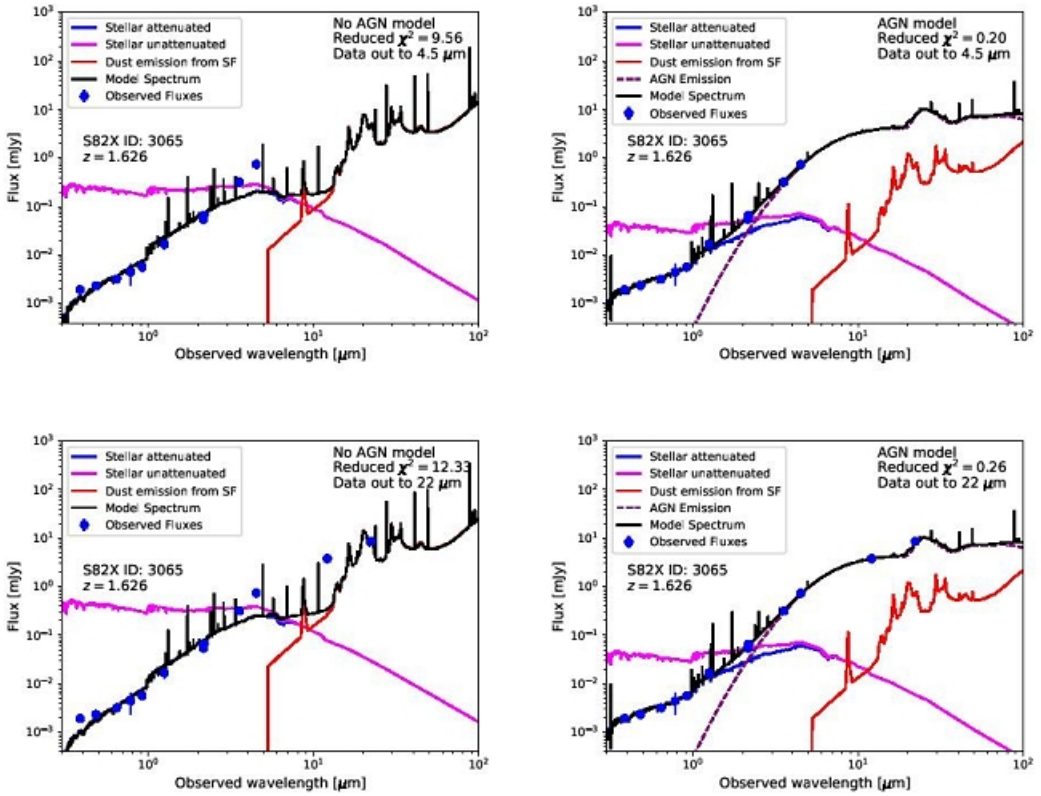

Figure 3. This figure compares model SED fits for a galaxy, whose redshift and Stripe 82X ID is displayed in each panel, with a type II X-ray luminous AGN in our samples S1-Lum-AGN (top two panels, with data coverage out to 4.5 μm and S1-Lum-AGN-WISE (bottom two panels with data coverage out to 22 μm) for SED fits that do not include AGN emission (left) and include AGN emission (right). The final model SED fit (solid black line) with AGN emission (right) is made up of the attenuated stellar emission (blue; which is inferred from the unattenuated stellar emission (magenta)), the dust emission from dust heated by massive stars from recent SF (red), the combined AGN emission (purple) from the accretion disk (particularly important at UV+optical wavelengths) and the dusty torus (particularly important at the 3 – 1000 μm wavelength range). The best-fit model SED without AGN emission (left) clearly cannot provide a good fit to the observed fluxes at wavelengths past 1 μm, therefore, the AGN emission templates are needed in order to constrain all emission above 1 μm. While WISE data at 12 and 22 μm can provide important constraints on the SED at longer wavelengths, a comparison of the top and bottom right panels of Figure 3 shows that for the galaxy fitted here, the IRAC 3.6 and 4.5 μm photometry alone, without any WISE photometry, can provide important constraints on the SED fits with AGN emission templates.

Таки да, в галактиках с активными ядрами звездообразование активнее

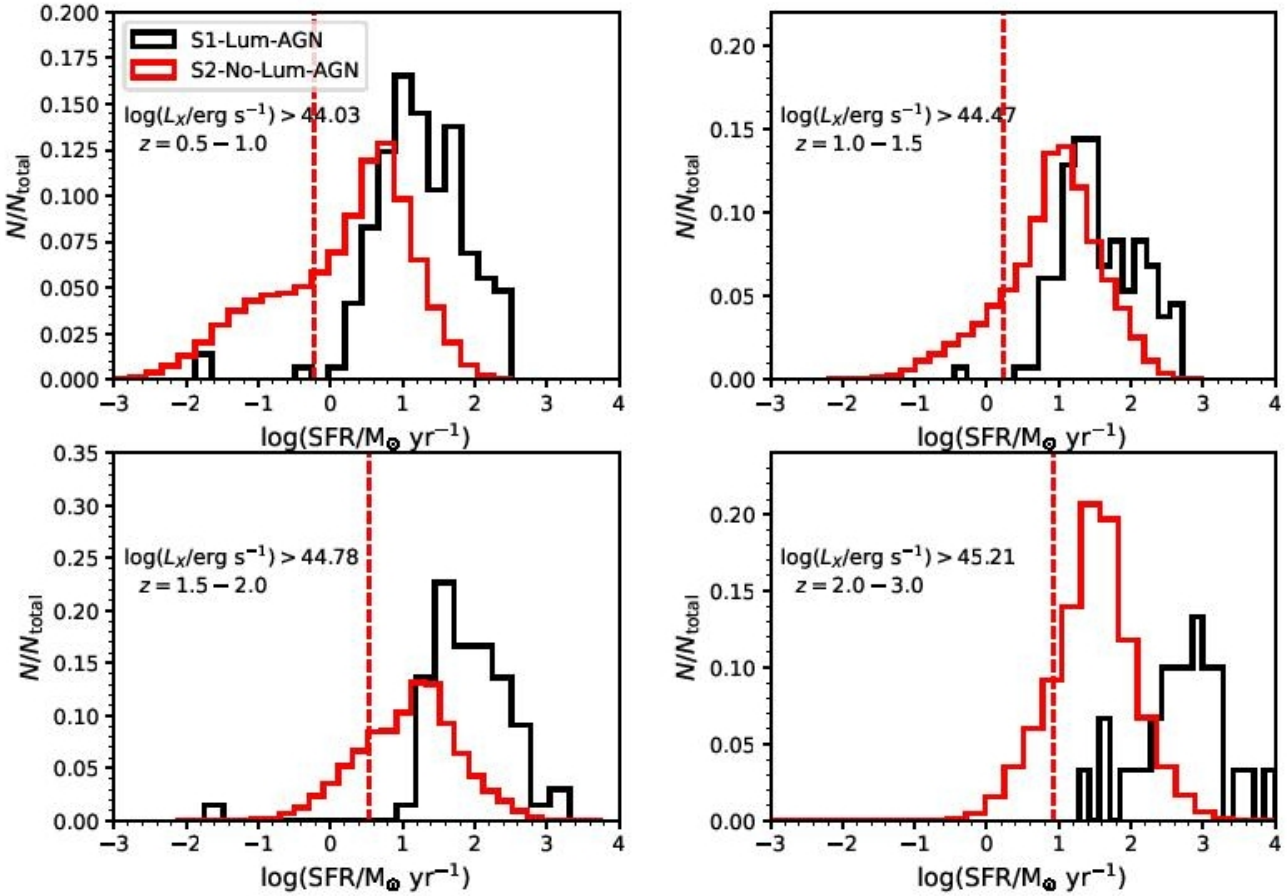

…в том числе, при фиксированной массе галактики

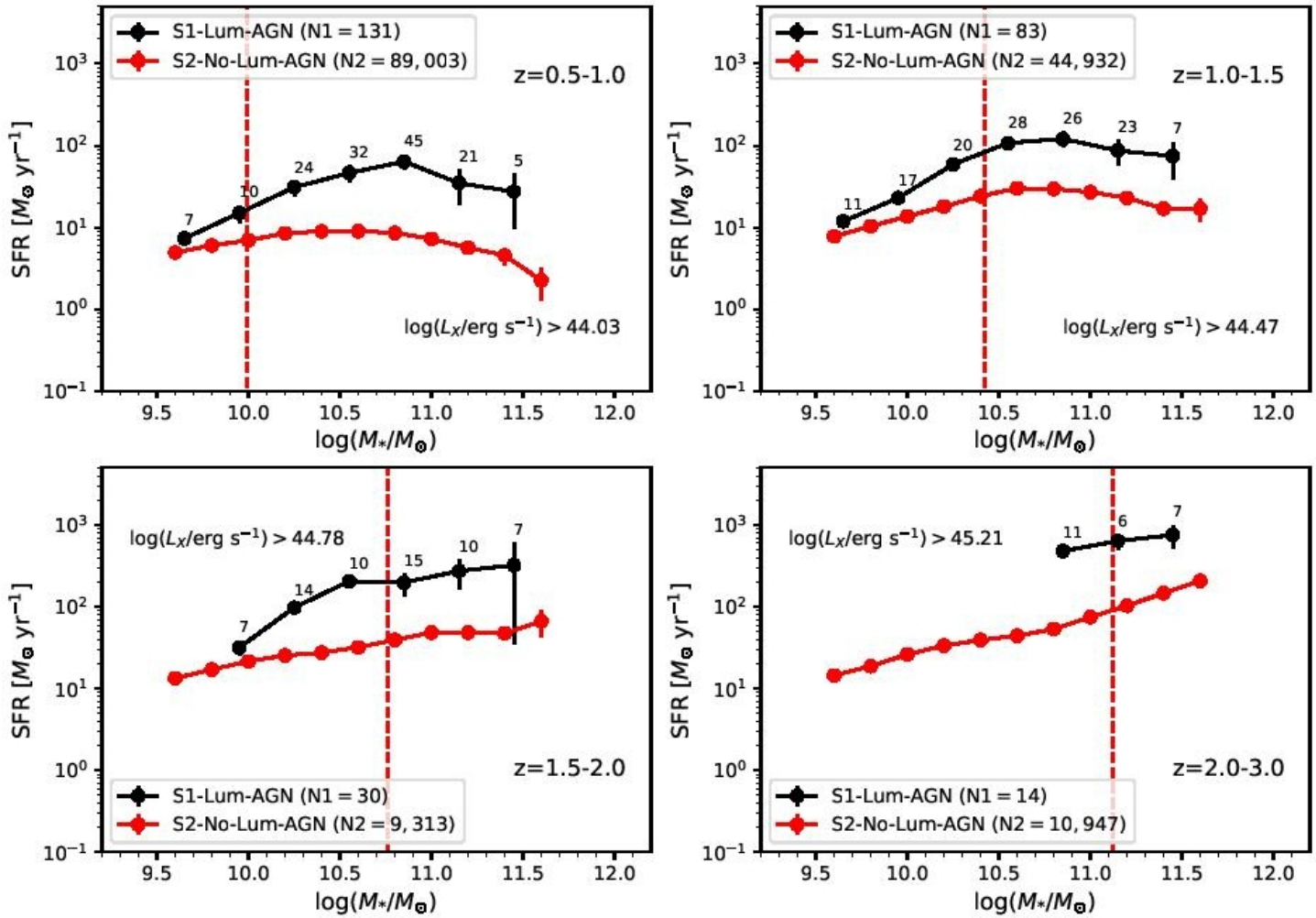

А где же quenched by AGN?

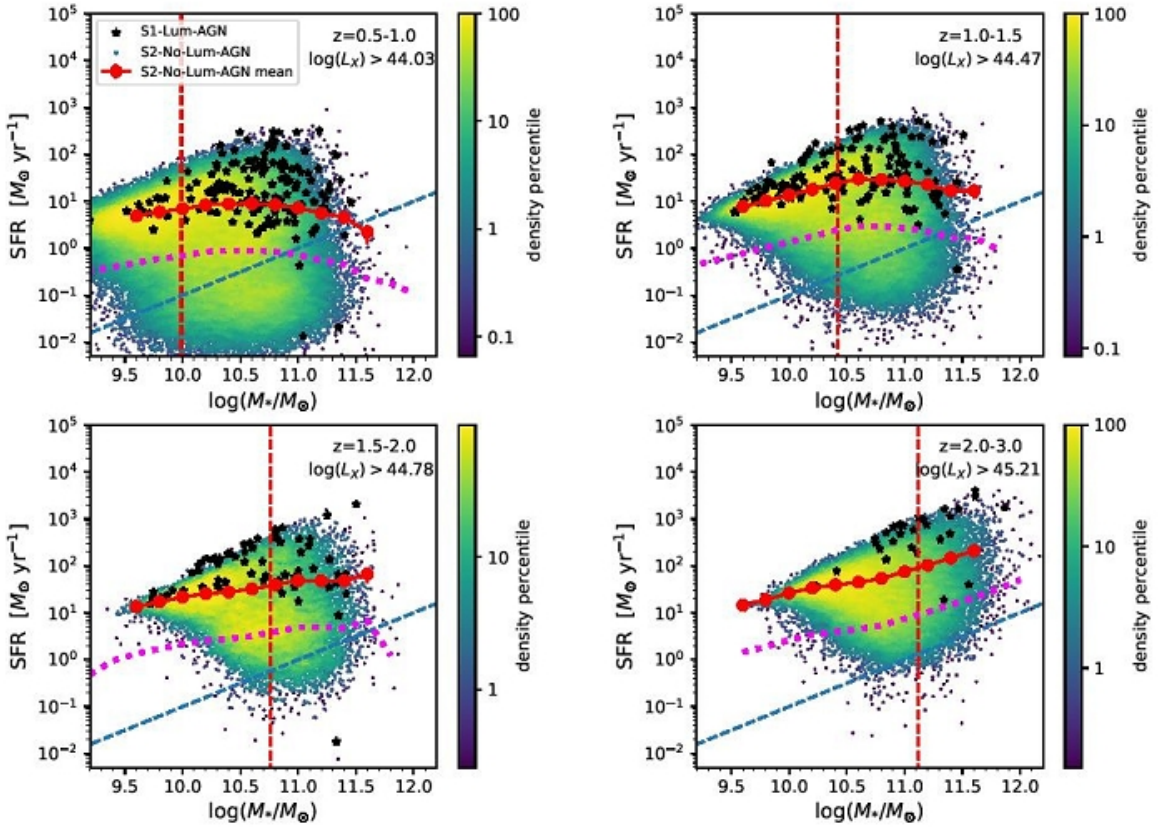

Figure 10. SFR vs. stellar mass for our sample of galaxies with (S1-Lum-AGN, black stars) and without (S2-No-Lum-AGN, colored points) X-ray luminous AGN in four different redshift bins. The S2-No-Lum-AGN galaxies are color-coded by their density on the stellar mass-SFR plane (see text). The dashed vertical line on each panel shows the stellar mass completeness limit in that bin (see Section 4.1). The X-ray completeness limit for S1-Lum-AGN is shown in each redshift bin in log units of ergs per second. Also shown are the mean SFR of S2-No-Lum-AGN as a function of stellar mass (red circles), which we refer to as the main sequence, the line that falls 1 dex below the main sequence (dotted magenta) and the line where the specific SFR is $10^{-11}\mathrm{yr}^{-1}$ (blue dashed). It is striking that galaxies with X-ray luminous AGN have higher mean SFRs than galaxies without X-ray luminous AGN at a given stellar mass (see also Figure 11). Note also that very few galaxies with X-ray luminous AGN have quenched SF if we use the common definition of quenched galaxies as having a specific SFR $< 10^{-11}\mathrm{yr}^{-1}$.

В галактиках с AGN их меньше, чем БЕЗ AGN!

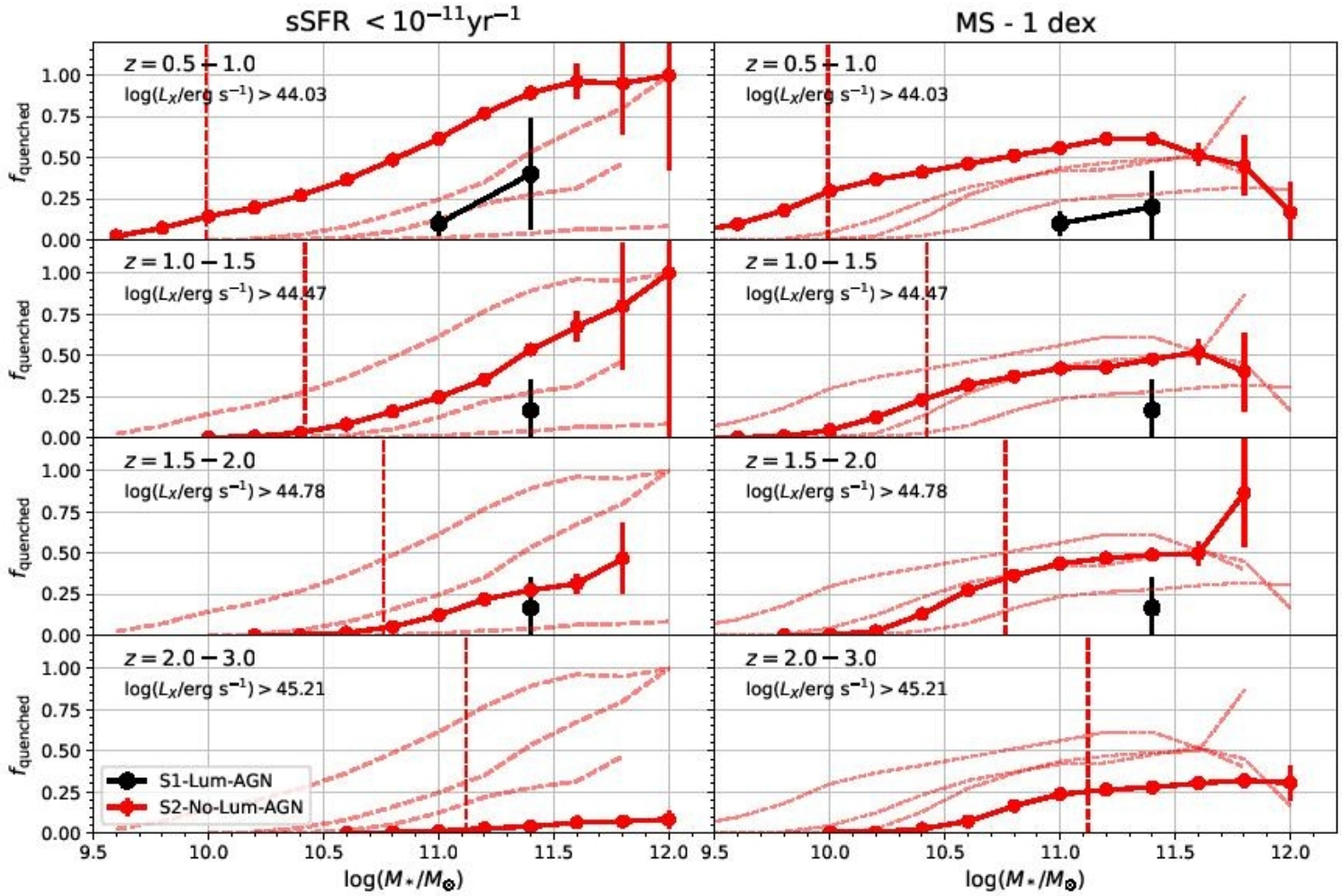

ArXiv: 2007.11285

Black Hole Accretion Correlates with Star Formation Rate and Star Formation Efficiency

MING-YANG ZHUANG,[1,2] LUIS C. HO,[1,2] AND JINYI SHANGGUAN[3]

[1]*Kavli Institute for Astronomy and Astrophysics, Peking University, Beijing 100871, China*
[2]*Department of Astronomy, School of Physics, Peking University, Beijing 100871, China*
[3]*Max-Planck-Institut für extraterrestrische Physik, Gießenbachstr. 1, D-85748 Garching, Germany*

Submitted to ApJ

ABSTRACT

We investigate the relationship between black hole accretion and star formation in a sample of 453 $z \approx 0.3$ type 1 active galactic nuclei (AGNs). We use available CO observations to demonstrate that the combination of nebular dust extinction and metallicity provides reliable estimates of the molecular gas mass even for the host galaxies of type 1 AGNs. Consistent with other similar but significantly smaller samples, we reaffirm the notion that powerful AGNs have comparable gas content as nearby star-forming galaxies and that AGN feedback does not deplete the host of cold gas instantaneously. We demonstrate that while the strong correlation between star formation rate and black hole accretion rate is in part driven by the mutual dependence of these parameters on molecular gas mass, the star formation rate and black hole accretion rate are still weakly correlated after removing the dependence of star formation rate on molecular gas mass. This, together with a positive correlation between star formation efficiency and black hole accretion rate, may be interpreted as evidence for positive AGN feedback.

SFR – через эмиссию [OII]3727

While polycyclic aromatic hydrocarbons closely trace ultraviolet photons from young stars (Shipley et al. 2016; Xie & Ho 2019), they can be destroyed by the more intense, harder radiation field of AGNs (Li 2020). Many attempts have been made to derive more reliable SFR diagnostics in AGNs, ranging from developing more sophisticated models of the IR emission from AGNs (e.g., Hönig & Kishimoto 2017; Lyu & Rieke 2017; Stalevski et al. 2019), improving the methods for fitting the spectral energy distribution (e.g., Ciesla et al. 2015; Yang et al. 2020), and devising empirical calibrations based on certain diagnostic emission lines (e.g., Ho 2005; Meléndez et al. 2008; Pereira-Santaella et al. 2010; Davies et al. 2016; Thomas et al. 2018). Building upon Ho & Keto (2007), Zhuang et al. (2019) used photoionization models based on realistic AGN spectral energy distributions and physical properties of the narrow-line region to calibrate a new SFR estimator for AGNs based on the mid-IR fine-structure lines of [Ne II] 12.81 μm, [Ne III] 15.55 μm, and [Ne V] 14.32 μm. The same set of models was then extended by Zhuang & Ho (2019) to the optical lines of [O II] λ3727 and [O III] λ5007, updating the prior effort of Kim et al. (2006).

А молекулярный газ – через пыль

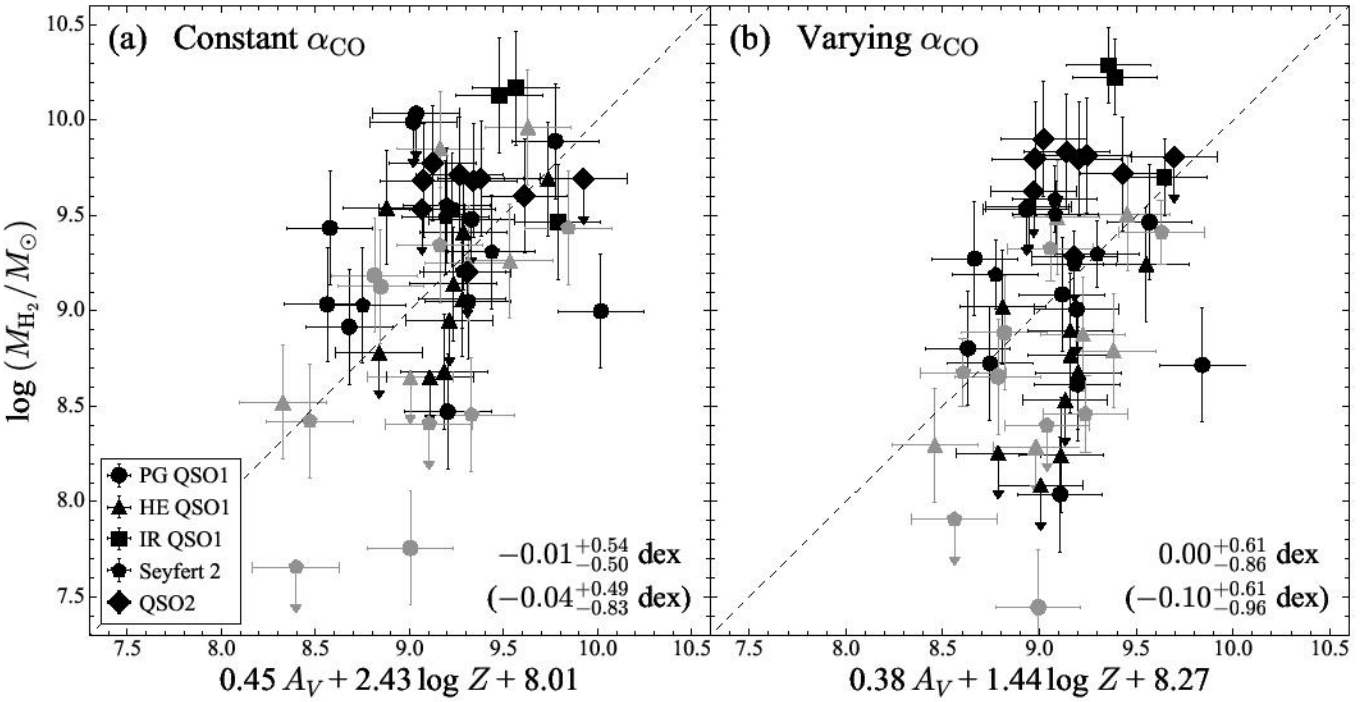

Figure 1. Comparison of molecular gas masses estimated from CO(1–0) measurements with those estimated from dust extinction and metallicity (Yesuf & Ho 2019), assuming (a) constant and (b) varying CO-to-H_2 conversion factor α_{CO}. We assume a constant $\alpha_{CO} = 3.1\ M_\odot$ (K km s^{-1} pc^2)$^{-1}$ for the Palomar-Green (PG) quasars, Hamburg/ESO (HE) quasars, and Seyfert 2 galaxies; for the IR-luminous quasars and type 2 quasars, we adopt $\alpha_{CO} = 0.8\ M_\odot$ (K km s^{-1} pc^2)$^{-1}$. Varying α_{CO} is calculated following Accurso et al. (2017). Objects with optical spectroscopic coverage smaller than 2 kpc are in gray. The median and $\pm 1\,\sigma$ difference of the two molecular gas mass estimates $(y - x)$ for

И SF, и аккреция на активное ядро определяются массой газа

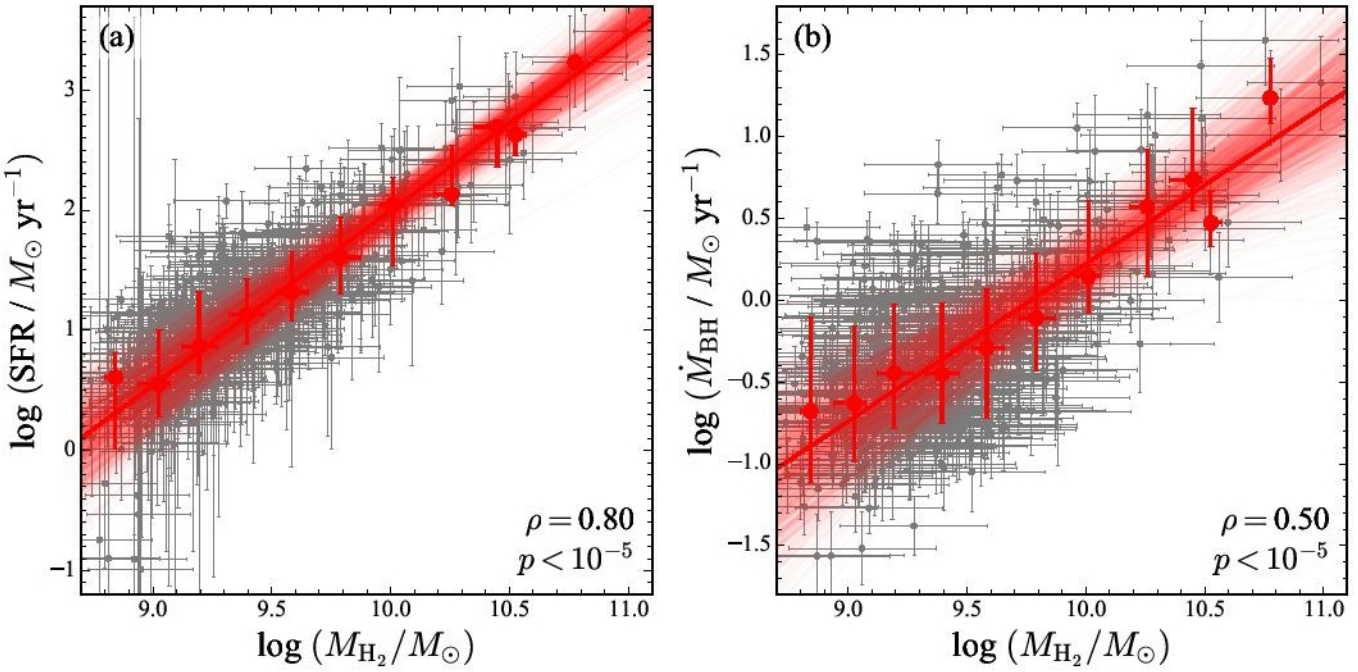

Figure 3. (a) Star formation rate and (b) BH accretion rate versus molecular gas mass for our $z = 0.3$ type 1 AGN sample. Small gray dots represent individual objects with errorbars indicating $1\,\sigma$ uncertainty. Large red dots indicate the median value in bins of 0.2 dex in M_{H_2}, with errorbars indicating 16th and 84th percentile. Fitting to the medians are visualized using the red lines. The Spearman correlation coefficients and p-values are given in the lower-right corner of each panel.

Но если убрать эту связь, все равно что-то остается: в галактиках с AGN SF активнее!

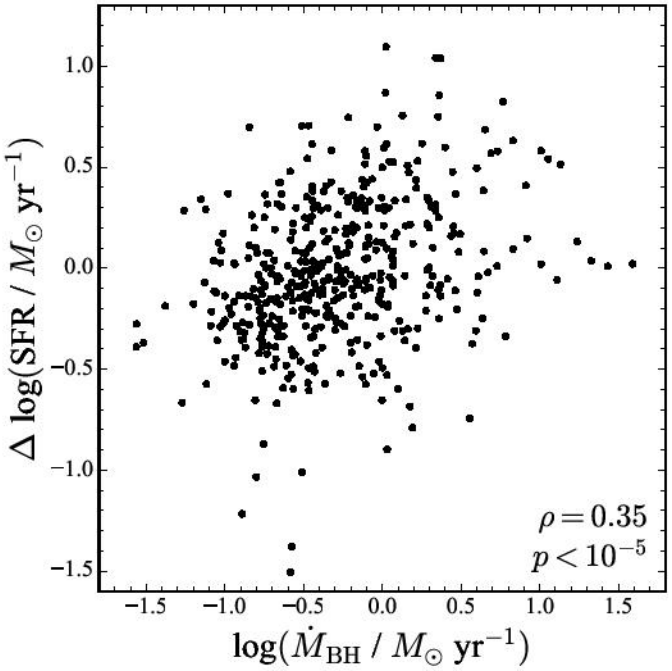

Figure 4. Star formation rate versus BH accretion rate after removing the dependence of SFR on $M_{\mathrm{H_2}}$ using Equation 3, for the sample of $z = 0.3$ type 1 AGNs. The Spearman correlation coefficient and p-value are shown in the lower-right corner.

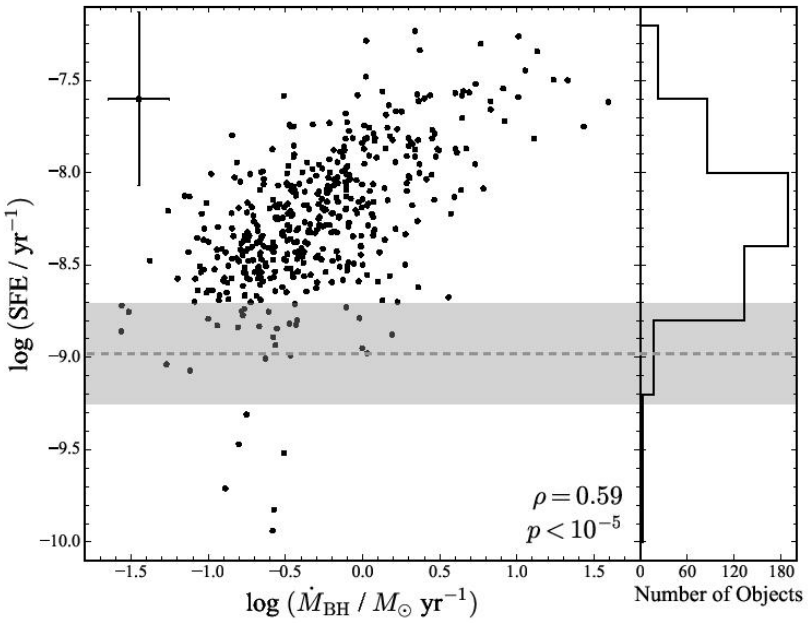

Figure 5. Star formation efficiency (SFE) versus BH accretion rate for $z = 0.3$ type 1 AGNs, with the histogram of SFE given in the right panel. Typical uncertainties are shown in the upper-left corner, and the Spearman correlation coefficient and p-value are shown in the lower-right corner. Gray dashed horizontal line represents the mean SFE of nearby main-sequence galaxies in Saintonge et al. (2017), with the shaded